Ab initio QM/MM Dynamics of H_3O^+ in Water

PATHUMWADEE INTHARATHEP, ANAN TONGRAAR, KRITSANA SAGARIK
School of Chemistry, Institute of Science, Suranaree University of Technology, 30000 Nakhon Ratchasima, Thailand

Received 18 December 2005; Revised 4 April 2006; Accepted 23 April 2006
DOI 10.1002/jcc.20503
Published online 10 August 2006 in Wiley InterScience (www.interscience.wiley.com).

Abstract: A molecular dynamics (MD) simulation based on a combined *ab initio* quantum mechanics/molecular mechanics (QM/MM) method has been performed to investigate the solvation structure and dynamics of H_3O^+ in water. The QM region is a sphere around the central H_3O^+ ion, and contains about 6–8 water molecules. It is treated at the Hartree-Fock (HF) level, while the rest of the system is described by means of classical pair potentials. The Eigen complex ($H_9O_4^+$) is found to be the most prevalent species in the aqueous solution, partly due to the selection scheme of the center of the QM region. The QM/MM results show that the Eigen complex frequently converts back and forth into the Zundel ($H_5O_2^+$) structure. Besides the three nearest-neighbor water molecules directly hydrogen-bonded to H_3O^+, other neighbor waters, such as a fourth water molecule which interacts preferentially with the oxygen atom of the hydronium ion, are found occasionally near the ion. Analyses of the water exchange processes and the mean residence times of water molecules in the ion's hydration shell indicate that such next-nearest neighbor water molecules participate in the rearrangement of the hydrogen bond network during fluctuative formation of the Zundel ion and, thus, contribute to the Grotthuss transport of the proton.

 J Comput Chem 27: 1723–1732, 2006

Key words: QM/MM; H_3O^+; Eigen; Zundel; proton transfer

Introduction

Characteristics of ions solvated in aqueous solutions have long been a topic of special interest for chemists and biologists in order to understand the role of these ions in chemical and biological processes.[1,2] Besides simple cations, the hydronium ion (H_3O^+) is one of the most fundamental ions, which has been widely used as a model system for understanding proton migration in liquid water[3–31] as well as proton transfer (PT) in proteins embedded in membranes.[32,33] One particularly interesting issue comes from the anomalously high mobility of protons in aqueous solution, compared with other cations.[34,35] To describe such fast proton mobility, a number of proton transport mechanisms[9–12,36–39] have been proposed. The mobility of protons in water has been generally regarded as a combination of protons jumping between different water molecules and diffusion of the entire protonated water complexes through the hydrogen bond network. The former type of proton transport process is much faster and is known as the Grotthuss structural diffusion mechanism,[40] in which the charge migration is characterized by successive jumps of proton from one oxygen site to the next; while in the latter type, the hydrated H_3O^+ complex diffuses through water in a way similar to other simple ions.

In experiments, attempts have been made to elucidate the microstructure as well as the dynamical properties of excess proton in water.[38,41,42] However, the behavior of the hydrated proton has not yet been clarified unambiguously, since it is rather difficult to prepare protonated water clusters for experimental observations. Furthermore, the structure of these clusters depends strongly on the neighboring water molecules.[43] Recently, the solvation structure of H_3O^+ in water has been examined experimentally using neutron diffraction with hydrogen isotope substitution.[44] It was found that each H^+ is part of a quite stable H_3O^+ ion which preferentially hydrogen-bonds to three nearest-neighbor water molecules. A fourth water molecule could be observed near the oxygen side of the H_3O^+ ion, exhibiting strong orientational correlations with the ion.

A number of theoretical studies have provided microscopic details on the nature of the H_3O^+ solvation, as well as on the mechanism of PT in water.[3–31] Based on theoretical investigations, it was postulated that the Eigen ($H_9O_4^+$) and Zundel ($H_5O_2^+$) complexes are the primarily important species in aqueous PT. Early computer simulations[10,11,17,45,46] indicated that the mechanism for PT in water involves a concerted double PT event, i.e., a conversion of one $H_5O_2^+$ moiety into another

Correspondence to: A. Tongraar; e-mail: anan@sut.ac.th

Contract/grant sponsor: The Thailand Research Fund under the Royal Golden Jubilee Ph.D. Program; contract/grant number: PHD/0225/2543

Contract/grant sponsor: The Thailand Research Fund under the TRF Basic Research Grant; contract/grant number: BRG4880010

directly, without a special involvement of H_3O^+. However, in recent Car-Parrinello (CP) path-integral simulations,[12] it was demonstrated that proton migration involves a concerted single PT event, i.e., the more stable H_3O^+ is converted into the slightly less stable $H_5O_2^+$ and *vice versa*. This interconversion is coupled to hydrogen bond dynamics in the second solvation shell of H_3O^+. With respect to the CP studies,[10–12] however, some methodical drawbacks might come from the use of a relatively small number of molecules in the simulation and from the quality of the density functionals employed in the calculation of the electronic structure. An empirical approach to describe the structural diffusion mechanism of PT is based on multistate empirical valence bond (MS-EVB) models,[15–21,24–26] which provide proton delocalization among several water molecules in a classical force field. In most recent MS-EVB studies,[20,21,23] it has been shown that H_3O^+ is more stable (longer living) than $H_5O_2^+$, and thus, the single PT event appears to be most probable. However, there are some significant differences between the simulation results using the MS-EVB potentials,[15–18,20–24,27] which were sensitive to the valence bond states employed in the models.[24]

An alternative approach to reach a reliable description of the structure and dynamics of hydrated H_3O^+ is to apply the so-called combined quantum mechanical/molecular mechanical (QM/MM) method. This QM/MM technique has been proved to be reliable for the studies of various condensed-phase systems,[47–57] providing new insights into composition, properties, and reactivity of the investigated systems. The QM/MM technique involves an (in principle highly accurate) *ab initio* treatment of the ion and its immediate environment, incorporating nonadditive and polarization effects into the description of the QM region, at the expense of a (less adequate) classical treatment of the MM region. In the present work, we have applied the QM/MM procedure to study the structure and dynamics of a single hydrated H_3O^+ in water at room temperature, using molecular dynamics (MD) simulation.

Method

The QM/MM technique[47–57] partitions the system into two parts, namely the QM and the MM region. The total interaction energy of the system is defined as

$$E_{\text{total}} = \langle \Psi_{\text{QM}} | \hat{H} | \Psi_{\text{QM}} \rangle + E_{\text{MM}} + E_{\text{QM-MM}}, \qquad (1)$$

where $\langle \Psi_{\text{QM}} | \hat{H} | \Psi_{\text{QM}} \rangle$ refers to the interactions within the QM region, while E_{MM} and $E_{\text{QM-MM}}$ represent the interactions within the MM and the coupling between the QM and MM regions, respectively. The QM region, which is the chemically most important region and includes the H_3O^+ ion and its surrounding water molecules, was treated by quantum mechanics, while the rest of the system was described by means of classical pair potentials. Based on this approach, the oxygen atom of H_3O^+ was regarded as the center of the QM region, in which water molecules were allowed to enter or leave during the QM/MM simulation, i.e., upon the defined distance between the hydronium oxygen and the oxygen atom of water molecules.

During the QM/MM simulation, the exchange of water molecules between the QM and MM regions can occur frequently. To keep the system energy constant, care must be taken that no jump in the forces occurs when a molecule enters or leaves the QM region. Thus, the forces acting on each particle in the system are interpolated continuously between quantum and molecular mechanics forces. This interpolation can be characterized through

$$F_i = S_m(r)F_{\text{QM}} + (1 - S_m(r))F_{\text{MM}}, \qquad (2)$$

where F_{QM} and F_{MM} are the QM and MM forces, respectively. $S_m(r)$ is a smoothing function,[58]

$$\begin{aligned} S_m(r) &= 1, && \text{for } r \le r_1, \\ S_m(r) &= \frac{(r_0^2 - r^2)^2 (r_0^2 + 2r^2 - 3r_1^2)}{(r_0^2 - r_1^2)^3}, && \text{for } r_1 < r \le r_0, \\ S_m(r) &= 0, && \text{for } r > r_0, \end{aligned} \qquad (3)$$

which acts in a narrow region between distances r_0 and r_1. r_0 and r_1 are two distances between the oxygen atoms of the H_3O^+ ion and of the water molecules, with $r_0 - r_1 = 0.2$ Å.

The reliability of the QM/MM results, besides the statistical requirement of a sufficiently long simulation trajectory for adequately sampling phase space, depends crucially on the QM level of theory, i.e., whether or not electron correlation is taken into account, on the choice of the basis set, and on the size of the QM region. In general, the inclusion of electron correlation in QM calculations can substantially improve the quality of the results. In practice, however, this procedure is extremely time-consuming. To estimate the effects of electron correlation, geometry optimizations of the H_3O^+–$(H_2O)_3$ complex were conducted using *ab initio* calculations at different levels of theory. The optimized structures and binding energies, calculated at the HF and several correlated levels as well as with the B3LYP density functional employing the D95(d,p) basis set[59,60] and using basis set superposition error (BSSE) correction,[61] are summarized in Table1. The D95(d,p) basis set was chosen, since it was also employed in the QM/MM simulation. Moreover, it is known that the use of larger basis set is a key factor for obtaining better results, i.e., closer to experimental data. However, the increase of basis set's size in the QM calculations requires more (too much) CPU time. In this work, the D95(d,p) basis set was considered to be large enough with respect to the available com-

Table 1. Structures and Binding Energies of Optimized H_3O^+–$(H_2O)_3$ Complex, Calculated at HF, B3LYP, and Higher Correlated Methods Using D95(d,p) Basis Set.

Method	ΔE (kcal mol^{-1})	∠HOH (°)	O—H (Å)	O—O (Å)
HF	−76.917	112.90	1.03	2.56
B3LYP	−90.365	114.19	1.02	2.54
MP2	−82.696	113.08	1.01	2.55
MP4	−79.580	113.29	1.00	2.56
CCD	−79.403	113.25	1.00	2.56
CID	−80.737	114.26	0.99	2.56

O—H and ∠HOH denote the geometry of H_3O^+ and O—O refers to the distance between the oxygen atom of H_3O^+ and of water.

putational facility. In terms of binding energies, an order of HF > MP4 ≈ CCD ≈ CID > MP2 > B3LYP was observed. In comparison with the results of the highly correlated methods, the neglect of electron correlation at the HF level results in a slight weakening of the binding energies. In contrast, the B3LYP calculations, although they provide reasonable geometries, predict too strong ion-water interactions, most probably due to an overestimation of the correlation energy.[54,56] From the data shown in Table 1, the contributions of electron correlation to the binding energies were estimated to be about 5%. This can be expected to have a significant influence on structural and dynamical properties of hydrated H_3O^+. However, in light of the fact that the computational expense even for the simplest correlated method (MP2) is significant, we decided to limit ourselves to the HF level and instead chose a larger size of the QM region. In addition, it has been shown, in a recent QM/MM simulation of pure water,[57] that the HF method with a sufficiently large QM region could provide detailed information of pure water in good agreement with the MP2 simulation.

For the QM size, we chose a QM diameter $d = 2r_1$ of 7.6 Å. This QM region includes the complete first hydration shell of H_3O^+ (i.e., the ion plus 3–4 water molecules) and some (about 3–4) next nearest-neighbor water molecules. For the interactions within the MM region and between the QM and MM regions, a flexible water model,[62,63] which describes inter- and intramolecular interactions, was employed. The pair potential function for describing H_3O^+–H_2O interactions was newly constructed. Total of 4056 MP2 interaction energy points for various H_3O^+–H_2O configurations were obtained from Gaussian98[64] calculations using the aug-cc-pvtz basis set.[65–67] The analytical form

$$\Delta E_{H_3O^+-H_2O} = \sum_{i=1}^{4}\sum_{j=1}^{3}\left[\frac{A_{ij}}{r_{ij}^6} + \frac{B_{ij}}{r_{ij}^8} + C_{ij}\exp(-D_{ij}r_{ij}) + \frac{q_iq_j}{r_{ij}}\right], \quad (4)$$

was fitted to these data points with fit parameters A, B, C, and D (see Table 2). r_{ij} denotes the distances between the i-th atom of H_3O^+ and the j-th atom of a water molecule, q_i and q_j are atomic net charges. The Mulliken charges on O and H of H_3O^+ were obtained from the *ab initio* calculation using aug-cc-pvtz basis set, and the charges on O and H of water were adopted from the flexible water model.[62,63] They were set to −0.0861, 0.3617, −0.6598, and 0.3299, respectively. The use of Mulliken charges, for the Coulombic terms in the construction of potential function, is one of acceptable procedures employed in almost all of such investigations published over the past decades.[47–57] It is known that through ion-water interactions these values change, but this effect will partially be compensated by the other terms in the potential during fitting to the MP2 energy surfaces. In this work, note that the short-range part of this potential ($r < 3.8$ Å) is not used because of our choice of r_1. In the sense that one should include as much as possible the physical effect into the newly developed potential model, other alternative approaches, i.e., ESP fitting or NBO analysis, are recommended.

Table 2. Optimized Parameters of the Analytical Pair Potential for the Interaction of Water with H_3O^+ (Interaction Energies in kcal mol^{-1} and Distances in Å).

Pair	A (kcal mol^{-1} Å^6)	B (kcal mol^{-1} Å^8)	C (kcal mol^{-1})	D (Å^{-1})
O_{hy}–O_w	13765.0507	−24306.2865	−1855.9251	1.5601
H_{hy}–O_w	262.9355	−138.8278	−2112.6279	2.9810
O_{hy}–H_w	149.5560	−128.6074	−2.9463	0.5078
H_{hy}–H_w	−30.9738	16.3171	1212.4652	3.8320

The QM/MM simulation was performed in the canonical ensemble at 298 K. The cubic box with box length of 18.17 Å contains one H_3O^+ and 199 water molecules. Periodic boundary conditions were applied, and the reaction-field method[68] was employed for the treatment of long-range interactions. The time step of 0.2 fs is short enough to describe the movement of hydrogen atoms of H_3O^+ and water adequately. The system was initially equilibrated by performing an MD simulation with a classical pair potential over 200,000 time steps. Then, the QM/MM simulation was started. The system was re-equilibrated for 20,000 time steps. This was followed by a simulation of 100,000 time steps, where configurations were collected for analysis at every 10th step.

Results and Discussion

Structural Properties

Since the detailed information on the solvation structure of hydrated H_3O^+ is crucial for understanding the proton transport dynamics, it is of particular interest to characterize the structural properties of the complex. Our QM/MM results for the O_{hy}—O_w and O_{hy}—H_w radial distribution functions (RDFs), together with their corresponding integration numbers, are shown in Figures 1a and 1b, respectively. Note that the subscripts "hy" and "w" in this article refer to hydronium ion and water molecule, respectively. The QM/MM simulation shows a sharp first O_{hy}—O_w peak with maximum at 2.6 Å. Integration of this peak up to the first O_{hy}—O_w minimum yields an average coordination number of 3.4, which implies the prevalence of a well-defined Eigen ($H_9O_4^+$) structure which is occasionally distorted because of the presence of the fourth water molecule in the first hydration shell. The coordination number observed in this work is in good accord with the recent experiment,[44] which demonstrated that, besides the three-coordinate nature of H_3O^+, a fourth water molecule can be found occasionally in the vicinity of the hydronium oxygen. Our first O_{hy}—O_w peak is in contrast to the results from earlier CP-MD and MS-EVB MD simulations,[10,18] which reported a splitting of the first O_{hy}—O_w peak due to the coexistence of the $H_9O_4^+$ and $H_5O_2^+$ complexes. It has been well-established that the PT process is an extremely fast dynamics process (e.g., the interconversion period between Eigen and Zundel hydration structure is only 1 ps or less), with Zundel form being the most important transition state complex. Interestingly, in the most recent CP-MD study,[31] no splitting was found in the first peak of O_{hy}—O_w RDF, which is consistent with the present QM/MM simulation. Thus, it is reasonable to conclude that the splitting of the first O_{hy}—O_w peaks reported in refs. 10 and 18 could

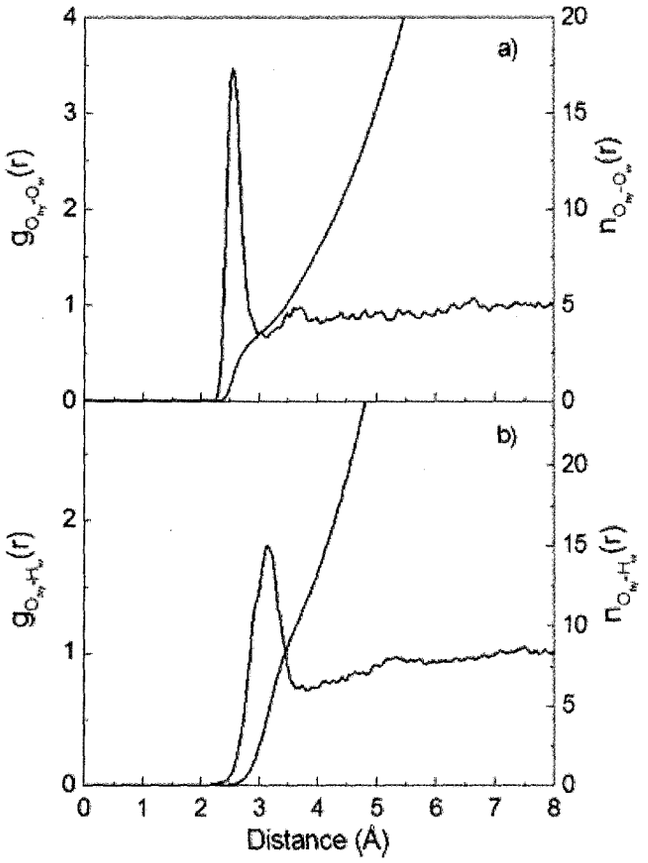

Figure 1. (a) O_{hy}—O_w and (b) O_{hy}—H_w radial distribution functions and their corresponding integration numbers.

be an indication that the models employed overestimated the stability of $H_5O_2^+$ formation. In other words, the $H_5O_2^+$ complex predicted in refs. 10 and 18 are too stable to represent a transition state complex in the PT process. According to the later CP-MD study,[31] however, the corresponding first O_{hy}—O_w peak was exhibited at a distance of about 2.5 Å, which was 0.1 Å shorter than that observed in the present QM/MM simulation. In addition, the first solvation shell of H_3O^+ was predicted to be significantly more rigid, with the smaller coordination number of 3.1. In the QM/MM simulation, the first solvation shell, as seen in our O_{hy}—O_w RDF, is not well separated from the bulk region, suggesting that the exchange of water molecules between the first solvation shell and the bulk takes place frequently (see later). The observed differences between the QM/MM and CP-MD results could be attributed partly to the neglect of the electron correlation effects at the HF level of theory. On the other hand, it could also be regarded as a consequence of the approximations and the parameterizations of the DFT methods, which is well-known to predict slightly more rigid hydration shell of ions in solutions.[54,57] In Figure 1b, a small shoulder observed on the O_{hy}—H_w peak around 2.7–2.8 Å suggests a weak $O_{hy}\cdots H_w$ hydrogen bond interaction on top of the H_3O^+ ion. The QM/MM results also demonstrate that H_3O^+ is not strongly shared in a local tetrahedral network of water.

Figure 2 shows the probability distribution of the number of surrounding water molecules, calculated up to the first minimum of the O_{hy}—O_w RDF. The first hydration shell of H_3O^+ prefers a coordination number of 3. Nevertheless, it is obvious that about 1/3 of the configurations favor four nearest-neighbor water molecules. Experimental neutron and X-ray diffractions[69,70] also suggested the possibility of four nearest-neighbor water molecules for each H_3O^+, in which the fourth water molecule might be found in two possible orientations: a proton-donor or a charge-dipole orientation.

The distributions of water orientations around the ion are shown as the distribution of the cosine of the angle β between the O_{hy}—O_w distance vector and the dipole vector of the H_3O^+ ion (Fig. 3). The QM/MM simulation shows a slight feature, almost constant distribution of orientations. This indicates again that the pyramidal H_3O^+ is not involved in a local tetrahedral

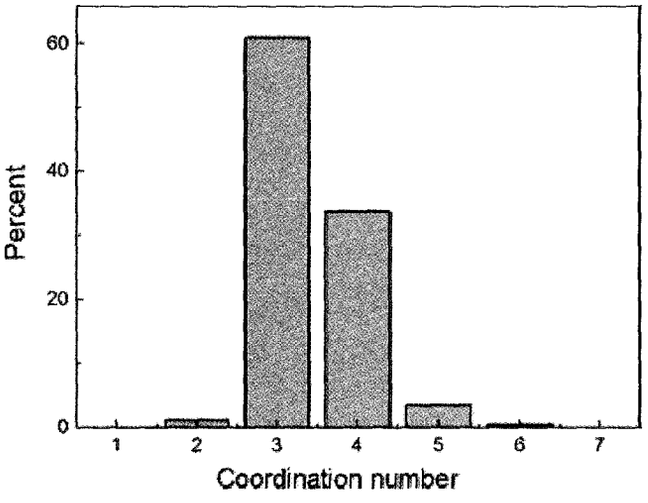

Figure 2. Distributions of coordination number, calculated up to an O_{hy}—O_w distance of 3.2 Å.

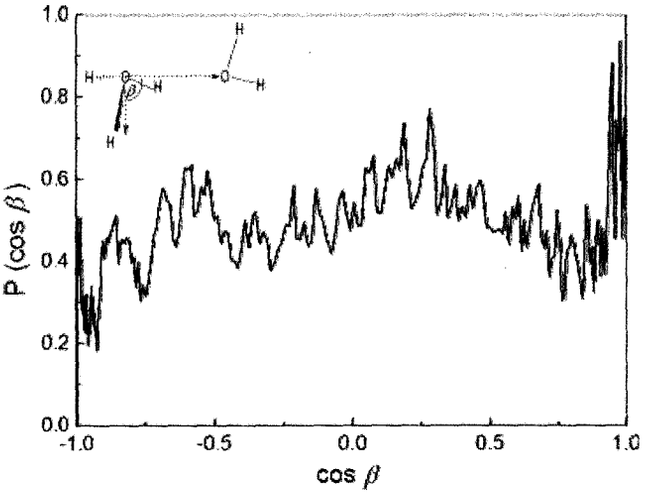

Figure 3. Distribution of the angle β between the instantaneous "symmetry" axis of the hydronium ion and the O_{hy}—O_w distance vector, for O_{hy}—O_w distances $\leq$3.2 Å.

structural motif and that the hydrogen bond structure is not particularly rigid. The absence of the fourth water molecule weakly bound in the lone pair direction of the H_3O^+ ion has been observed in the structures of the optimized $(H_2O)_5H^+$ cluster.[6]

Information on the hydrogen bond characteristics between H_3O^+ and water can be obtained from the H_{hy}—O_w and H_{hy}—H_w RDFs, as shown in Figure 4. The QM/MM simulation shows the first H_{hy}—O_w peak with a maximum at 1.53 Å, which is attributed to the hydrogen bonds between the hydronium hydrogens and their nearest-neighbor water molecules. The integration up to the first minimum of the H_{hy}—O_w RDF yields one (1.02) well-defined hydrogen bond between a water molecule and each hydrogen atom of the H_3O^+ ion. In the recent CP-MD study,[31] the corresponding H_{hy}—O_w peak exhibited, again, at a distance around 0.1 Å was shorter than that observed in the QM/MM simulation. This discrepancy can be explained using the same arguments as in the case of O_{hy}—O_w RDF. In Figure 4b, the H_{hy}—H_w RDF shows a pronounced first peak at 2.14 Å, which is consistent with the resulting H_{hy}—O_w RDF.

For more detailed analysis of hydrogen bonding between H_3O^+ and water molecules, the probability distributions of the cosine of the O_{hy}—$H_{hy}\cdots O_w$ angle (calculated from the subset of configurations with H_{hy}—O_w distances smaller than 2.0 (dashed) and smaller than 2.5 Å (full line), respectively), are plotted in Figure 5. The

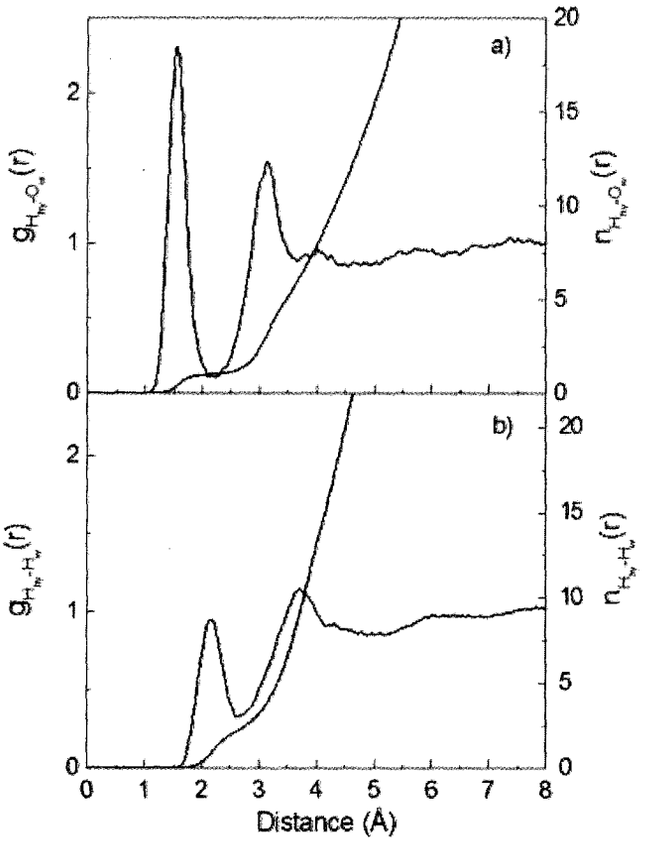

Figure 4. (a) H_{hy}—O_w and (b) H_{hy}—H_w radial distribution functions and their corresponding integration numbers.

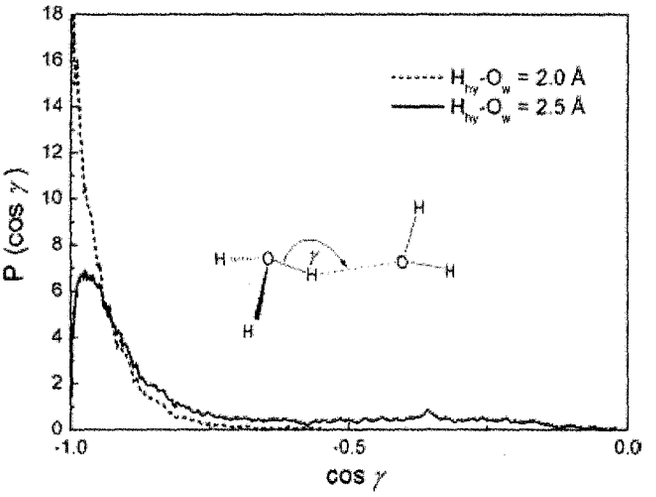

Figure 5. O_{hy}—H_{hy}—O_w angular distributions as indicated, calculated for H_{hy}—O_w distances $\leq$2.0 and $\leq$2.5 Å, respectively.

overall short H_{hy}—O_w distances of less than 2.2 Å (the first minimum of the H_{hy}—O_w RDF in Fig. 4) are consistent with almost linear O_{hy}—$H_{hy}\cdots O_w$ hydrogen bonds. Comparing between the two curves, deviation of the curve at slightly longer H_{hy}—O_w distance of 2.5 Å can be attributed to the presence of the next nearest-neighbor (e.g., the fourth) water molecule.

Figure 6 shows the distribution of the cosine of the angle θ between the H_{hy}—O_w vector and the dipole vector of the hydration water molecules. The QM/MM simulation shows a clear dipole-oriented arrangement of nearest-neighbor water molecules towards H_3O^+. In addition, a small maximum is observed around cos θ = 0.7, which could be attributed to the correlations between the next nearest-neighbor water molecules and the lone pair direction.

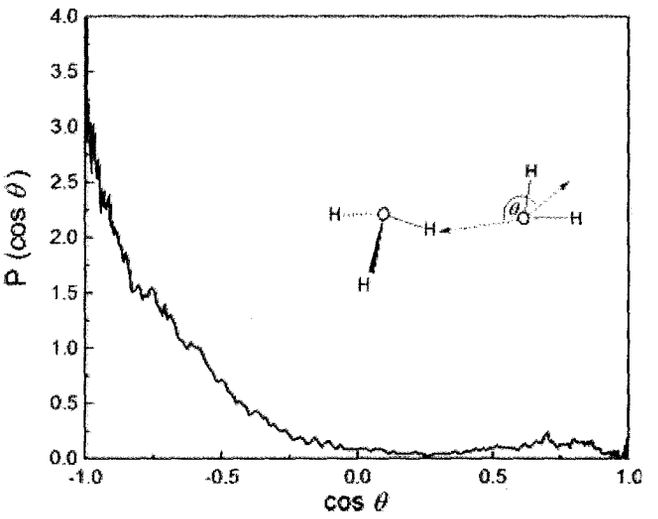

Figure 6. Distributions of the angle θ, between the intramolecular OH vector and the water dipole vector, for O_{hy}—O_w distances $\leq$3.2 Å.

Intramolecular Geometry

The intramolecular geometry of the H_3O^+ ion and of the first shell water molecules is described by the distributions of their O—H bond lengths and H—O—H angles in Figure 7. Both the O—H and H—O—H distributions of H_3O^+ are broader than those of the first shell water molecules. This is an indication of the partial formation of $H_5O_2^+$, in which the intramolecular O_{hy}—H_{hy} bond is fully extended at the expense of a short O_w—H_{hy} distance.

Figure 8 shows the corresponding probability distributions of the *longest* intramolecular O_{hy}—H_{hy} bond distance (full line) which is obtained by choosing the longest O_{hy}—H_{hy} bond in each analyzed configuration. It shows a maximum peak around 1.1 Å, which is very close to the corresponding distance of the symmetrical Zundel ion, and ranges up to 1.3 Å. At the same time, the distribution of the shortest intermolecular O_w—H_{hy} distance also shows a maximum around 1.45 Å and ranges down to about 1.15 Å. The overlap of the two distributions corresponds to (almost) symmetrical Zundel ions. Note that, because of the structure of H_3O^+ adopted at the beginning of the simulation, completely symmetric Zundel structures are not allowed.

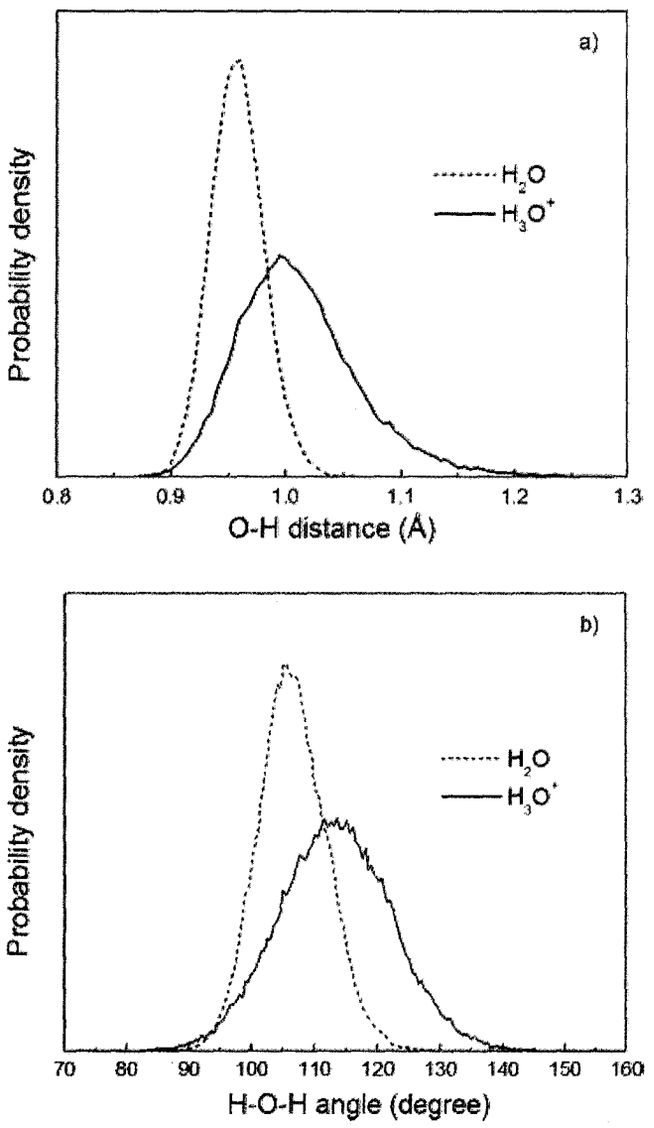

Figure 7. Distributions of (a) bond lengths and (b) bond angles between H_3O^+ and the nearest-neighbor water molecules.

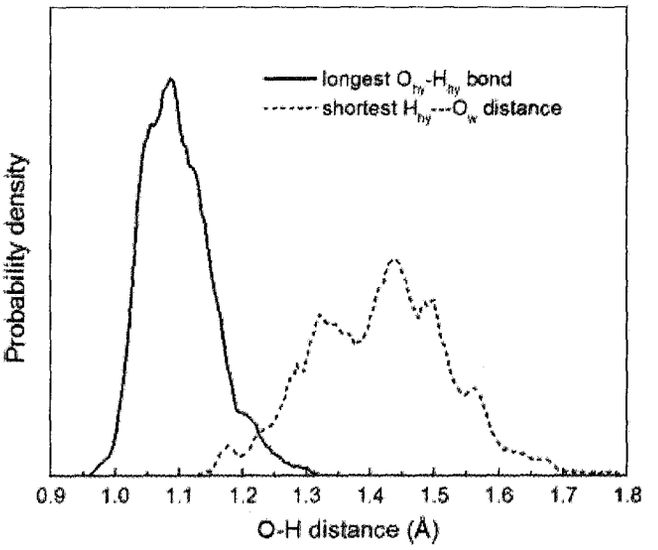

Figure 8. Distributions of the longest intramolecular O_{hy}—H_{hy} bond length (full line) and of the shortest intermolecular $H_{hy}\cdots O_w$ distance (dashed).

Dynamical Properties

Translational Motions

The self-diffusion coefficient (SDC) D was calculated from the center-of-mass velocity autocorrelation function (VACF) $C_v(t)$ for H_3O^+ using the Green-Kubo relation,[71]

$$D = \frac{1}{3}\lim_{t\to\infty}\int_0^t C_v(t)\,dt. \tag{5}$$

Integrating the VACF over 2.0 ps yields an estimate for D of 9.9×10^{-5} cm^2 s^{-1}. This value (at 'infinite' dilution) seems to be in good agreement with the experimentally observed proton diffusion coefficient of 9.3×10^{-5} cm^2 s^{-1} (at high concentration and in the presence of counterions).[9] By the way, remarks should be made on the diffusion coefficient obtained by the present QM/MM simulation. It is recognized that the total proton conductivity (vehicle mechanism[72]) in aqueous solution results mainly from the diffusion of the protonated water (H_3O^+) and the Grotthuss mechanism. However, the relative contribution between the "vehicle" and "structure" diffusions seems not easy to identify.[73] In addition, because of the use of restricted QM region, the proton can oscillate between the H_3O^+ ion and water molecules in the first and some parts of the sec-

ond hydration shells. Such an oscillation can occur at a much faster rate (e.g., because of the very low barrier of PT reaction) than the Grotthuss transport that requires the protonic charge penetration coupling between the first and the second shell water molecules. Since the Grotthuss mechanism, together with the nuclear quantum effects, is not taken into account in the present QM/MM simulation, we anticipate that the observed D value could be somewhat overestimated.

The power spectrum, which corresponds to the hindered translation of H_3O^+ in water, was obtained by Fourier transformation of the center-of-mass VACF using the correlation length of 2.0 ps, with 2000 averaged time origins and is shown in Figure 9. The Fourier transformation shows two maxima. The first maximum at zero frequency signifies fast translational motion of the ion in water, while the second one at 360 cm^{-1} could be attributed to the fast H_3O^+ subunit motion during the formation and destruction of the transient $H_5O_2^+$ complex which is largely oscillatory in nature (see details in the Proton Transfer Dynamics section).

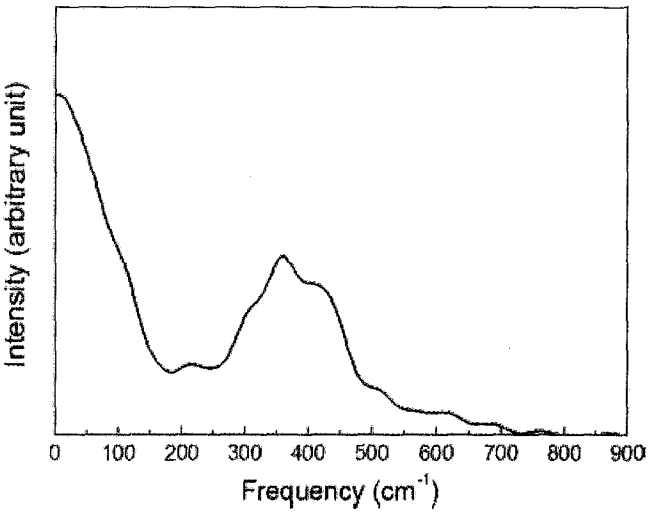

Figure 9. Fourier transform of the translational velocity autocorrelation function of the H_3O^+ ion in water.

Water Exchange in the Hydration Shell of H_3O^+

The exchange processes of water molecules near each of the hydronium hydrogen atoms can be best visualized by the plots of the H_{hy}—O_w distances against simulation time, as shown in Figure 10. In the course of the QM/MM simulation, several water exchange processes were observed at the hydronium hydrogens, most of which are associative exchange (A) and associative interchange (I_a) mechanisms. These types of exchange process are indicative of strong ion-water interactions.

The rate of water exchange processes at the hydronium hydrogens was evaluated through the mean residence time (MRT) of the water molecules. In this work, the MRT data were calculated using the direct method[74] with t^* values of 0.0 and 0.5 ps and the results are summarized in Table 3. The time parameter t^* has been defined as a minimum duration of the ligand's displacement from its original coordination shell. In general, the MRT data obtained using $t^* = 0.0$ ps are used as estimation of hydrogen bond lifetimes, whereas the data obtained with $t^* = 0.5$ ps can be considered as a good estimate for ligand exchange processes.[74] For $t^* = 0.0$ ps, the QM/MM simulation leads to widely varying MRT values, which are of the same order of magnitude as for pure water,[57] yet significantly distinct for each of the three hydrogen atoms, indicating the limitations of the QM/MM simulation with respect to the short simulation time. It could, however, imply an imbalance of the hydrogen-bond strength at each of hydronium hydrogens, due to the temporary formation of Zundel complexes. Comparing the bulk and the hydration shell dynamics of water molecules on the basis of the MRT is quite meaningful, since the MRT data for pure water were available based on a similar QM/MM simulation. Using a definition $t^* = 0.5$ ps, the QM/MM simulation clearly shows an order of $\tau_{H_2O}(H_i) > \tau_{H_2O}(H_2O)$ for all three hydrogen atoms of H_3O^+. In comparison to the MRT data for pure water,[57] the QM/MM simulation thus clearly indicates a "structure-making" ability of the H_3O^+ ion in aqueous solution.

Proton Transfer Dynamics

To study "chemical reactions" such as the PT in the solution of hydronium in water, bond breaking and forming within the hydrated H_3O^+ complex has to be accurately described. In aqueous solution, it is well-established that the $H_9O_4^+$ and $H_5O_2^+$ complexes are the most important species. $H_9O_4^+$ is formed when the three hydrogens in H_3O^+ are equivalently hydrated, forming three analogous hydrogen bonds with three nearest-neighbor water molecules. $H_5O_2^+$ is formed when one hydrogen atom of the ion is symmetrically shared with its hydrogen bonding water molecule. The properties of $H_5O_2^+$ have been investigated in quantum mechanical calculations of isolated $(H_2O)_nH^+$ clusters,[4–7] as well as in previous *ab initio* simulations.[10–12]

To obtain some information on the frequency of the $H_5O_2^+$ formation, threshold values for the O_{hy}—O_w distances (R_{max}) are established to monitor the $H_5O_2^+$ ion. The $H_5O_2^+$ complex is considered to be "formed" when the O_{hy}—O_w distance in the original $H_9O_4^+$ complex is smaller than R_{max}. For R_{max} = 2.4 Å (e.g., the equilibrium O—O distance of H_2O—H^+—OH_2 in gas-phase[9]), the QM/MM simulation reveals that ~10% of the MD configurations consists of the $H_5O_2^+$ structure. Increasing R_{max} to 2.5 Å, the proportion of $H_5O_2^+$ in solution rapidly increases to 45%. In addition, configurations such as $H_7O_3^+$ (i.e., a complex in which two of the O_{hy}—O_w distances of the original $H_9O_4^+$ are $\leq$2.5 Å), can also be observed, in about 10% of the cases. In fact, the $H_5O_2^+$ and $H_7O_3^+$ structures belong to the same fluctuating complex ($H_9O_4^+$), i.e., small shift of the hydronium hydrogen atoms along their O_{hy}—H_{hy} bonds converts the original $H_9O_4^+$ into either $H_7O_3^+$ or $H_5O_2^+$ structures, and *vice versa*.

During the simulation, charges of all particles within the QM region can vary dynamically. Consequently, transient interconversions between the H_3O^+-centered complex, $H_9O_4^+$, and the $H_5O_2^+$-centered Zundel form are accompanied by charge fluctuations. Figure 11 displays the variations of O_{hy}—H_{hy} bond length

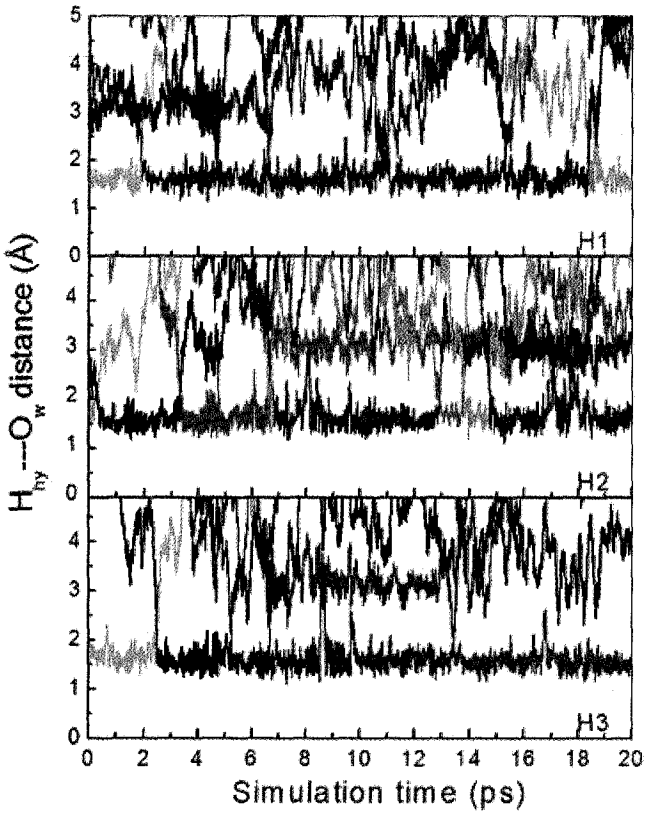

Figure 10. Time dependence of H_{hy}—O_w distances.

and H_{hy}—O_w distance over a short time span of 4 ps. There are only few situations in which the intramolecular O_{hy}—H_{hy} and the intermolecular H_{hy}—O_w distances are equal. Thus the symmetric $H_5O_2^+$ structure is expected to be not very stable (short-lived) in the current simulation, i.e., once the Zundel complex is formed, it rapidly reverts back to the original $H_9O_4^+$ complex. As a consequence, the first maximum of the O_{hy}—O_w RDF (Fig. 1a) is not split or significantly broadened. Interestingly, as can be seen from the trajectory around 2.5 ps, a water exchange process can simultaneously take place near one hydrogen (H3) as a consequence of an intermediate formation of the $H_5O_2^+$ around another hydrogen (H2). A similar process seems to occur at around 3.4 ps (H2 and H1).

Table 3. Mean Residence Time of Water Molecules in the Bulk and in the First Hydration Shell of the Hydronium Hydrogens, Calculated Within the First Minimum of H_{hy}—O_w RDF

			$t^* = 0.0$ ps		$t^* = 0.5$ ps	
Atom/solute	CN	t_{sim}	N_{ex}^0	$\tau_{H_2O}^0$	$N_{ex}^{0.5}$	$\tau_{H_2O}^{0.5}$
H1	1.0	20.0	65	0.31	8	2.50
H2	1.0	20.0	113	0.18	11	1.82
H3	1.0	20.0	47	0.42	8	2.50
Pure H_2O[57]	4.2	40.0	–	0.33	–	1.51

Based on the QM/MM results, the structure and dynamics of the hydrated H_3O^+ can be summarized as follow. Starting from a quite stable H_3O^+ ion, i.e., a structure in which the positive charge is localized at the center of the ion with three equivalent neighboring water molecules each of which forming a hydrogen bond, the $H_9O_4^+$ complex is formed. When the next nearest-neighbor water (e.g., the fourth water molecule) approaches the central oxygen atom of $H_9O_4^+$, it exchanges with one of the water molecules of the complex (at 2 ps in Fig. 10), leading to a perturbation of the charge distribution in the complex; which subsequently causes an imbalance of the partial charges at each of the hydronium hydrogens, and finally, to an imbalance of the H_{hy}—O_w hydrogen-bond distances. Under this circumstance, the strongest O_{hy}—H_{hy}—O_w bond (i.e., the one with the shortest O_{hy}—O_w distance) in the $H_9O_4^+$ complex transiently converts to the $H_5O_2^+$ intermediate and suddenly back to the $H_9O_4^+$ form.

Conclusion and Outlook

We have performed a combined QM/MM molecular dynamics simulation to study the solvation structure and dynamics of the H_3O^+ ion in water. Based on our QM/MM results, the $H_9O_4^+$ structure was found to be the most stable species in aqueous solution. Nevertheless, this complex can rapidly convert back and forth to a Zundel ion $H_5O_2^+$ (or, with lower probability, to an

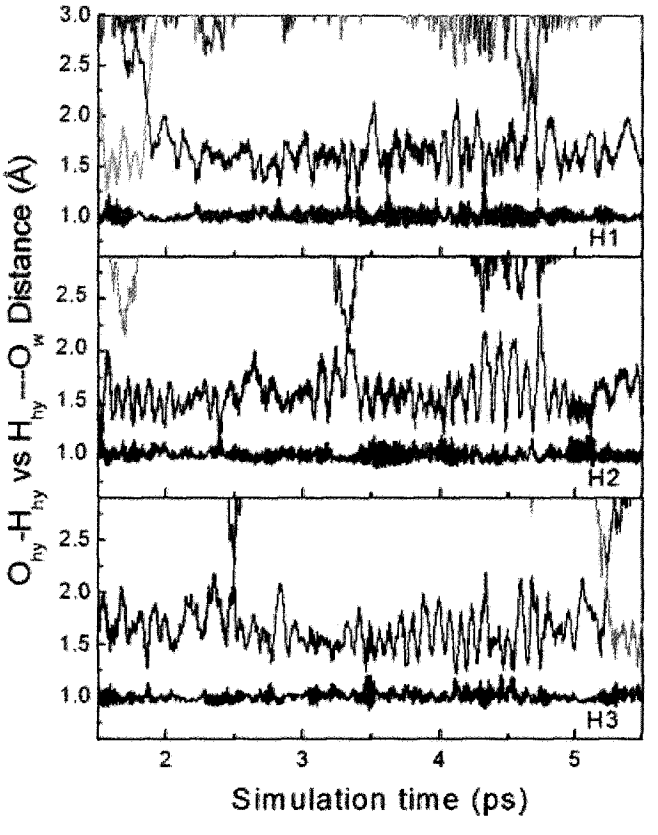

Figure 11. Time dependence of O_{hy}—H_{hy} bond lengths and H_{hy}—O_w distances for a 4-ps period.

$H_7O_3^+$ complex). During the simulation, it was observed that the next nearest-neighbor water, in particular the fourth water molecule, can approach the H_3O^+ ion quite closely, leading to a hydrogen bond formation as well as the water exchange, which could contribute significantly to the proton transport mechanism taking place along the hydrogen-bond network of bulk water.

A final remark should be made on our QM/MM results. By the QM/MM scheme, the use of restricted QM region allows the proton to oscillate only between the H_3O^+ ion and water molecules in the first and some part of the second hydration shells and, thus, no actual PT is allowed during the QM/MM simulation. In this context, the results obtained by the QM/MM simulation can provide detailed information with respect to the structure and dynamics of the hydrated H_3O^+ complex at the state "before" and/or "after" the actual PT process, rather than to visualize pathway of the PT. In an ongoing study, attempt is being made to improve our model, by increasing the radius of the QM sphere and investigate the effects of electron correlation on the reported structural and dynamical properties of the hydrated H_3O^+ complexes.

References

1. Richens, D. T. The Chemistry of Aqua Ions; Wiley: New York, 1997.
2. Frausto da Silva, J. J. R.; Williams, R. J. P. The Biological Chemistry of the Elements—The Inorganic Chemistry of Life; Oxford University Press: New York, 1991.
3. Ruff, I.; Frierich, V. J. J Phys Chem 1972, 76, 2954.
4. Kochanski, E. J Am Chem Soc 1985, 107, 7869.
5. Karlström, G. J Phys Chem 1988, 92, 1318.
6. Wei, D. Q.; Salahub, D. R. J Chem Phys 1994, 101, 7633.
7. Cheng, H. J Phys Chem A 1998, 102, 6201.
8. Christie, R. A.; Jordan, K. D. J Phys Chem A 2001, 105, 7551.
9. Agmon, N. Chem Phys Lett 1995, 244, 456.
10. Tuckerman, M. E.; Laasonen, K.; Sprik, M.; Parrinello, M. J Chem Phys 1995, 103, 150.
11. Tuckerman, M. E.; Laasonen, K.; Sprik, M.; Parrinello, M. J Phys Chem 1995, 99, 5749.
12. Tuckerman, M. E.; Marx, D.; Klein, M. L.; Parrinello, M. Science 1997, 275, 817.
13. Sagnella, D. E.; Tuckerman, M. J Chem Phys 1998, 108, 2073.
14. Marx, D.; Tuckerman, M. E.; Hutter, J. G.; Parrinello, M. Nature 1999, 397, 601.
15. Vuilleumier, R.; Borgis, D. J Mol Struct 1997, 436, 555.
16. Vuilleumier, R.; Borgis, D. Chem Phys Lett 1998, 284, 71.
17. Vuilleumier, R.; Borgis, D. J Phys Chem B 1998, 102, 4261.
18. Vuilleumier, R.; Borgis, D. J Chem Phys 1999, 111, 4251.
19. Lobaugh, J.; Voth, G. A. J Chem Phys 1996, 104, 2056.
20. Schmitt, U. W.; Voth, G. A. J Phys Chem B 1998, 102, 5547.
21. Schmitt, U. W.; Voth, G. A. J Chem Phys 1999, 111, 9361.
22. Brodskaya, E.; Lyubartsev, A. P.; Laaksonen, A. J Phys Chem B 2002, 106, 6479.
23. Day, T. J. F.; Soudackov, A. V.; Čuma, M.; Schmitt, U. W.; Voth, G. A. J Chem Phys 2002, 117, 5839.
24. Lapid, H.; Agmon, N.; Petersen, M. K.; Voth, G. A. J Chem Phys 2005, 122, 14506.
25. Wang, F.; Voth, G. A. J Chem Phys 2005, 122, 144105.
26. Brancato, G.; Tuckerman, M. E. J Chem Phys 2005, 122, 224507.
27. James, T.; Wales, D. J. J Chem Phys 2005, 122, 134306.
28. Hermida-Ramón, J. M.; Karlström, G. J Mol Struct 2004, 712, 167.
29. Kim, J.; Schmitt, U. W.; Gruetzmacher, J. A.; Voth, G.; Scherer, N. E. J Chem Phys 2002, 116, 737.
30. Day, T. J. F.; Soudackov, A. V.; Cuma, M.; Schmitt, U. W.; Voth, G. A. J Chem Phys 2002, 117, 5849.
31. Izvekov, S.; Voth, G. A. J Chem Phys 2005, 123, 044505.
32. Drukker, K.; de Leeuw, S. W.; Hammes-Schiffer, S. J Chem Phys 1998, 108, 6799.
33. Pomès, R.; Roux, B. J Phys Chem 1996, 100, 2519.
34. Robinson, R. A.; Stokes, R. H. Electrolyte Solutions, 2nd ed.; Butterworths: London, 1959.
35. Atkins, P. W. Physical Chemistry, 5th ed.; Freeman: New York, 1994.
36. Hückel, E. Elektrochem Angew Phys Chem 1928, 34, 546.
37. Bernal, J. D.; Fowler, R. H. J Chem Phys 1933, 1, 515.
38. Conway, B. E. Modern Aspects of Electrochemistry; Butterworths: London, 1964.
39. Eigen, M. Angew Chem 1964, 3, 1.
40. von Grotthuss, C. J. D. Ann Chim 1806, LVIII, 54.
41. Kebarle, P. Annu Rev Phys Chem 1977, 28, 445.
42. Giguere, P. A. Chem Phys 1981, 60, 421.
43. Headrick, J. M.; Diken, E. G.; Walters, R. S.; Hammer, N. I.; Christie, R. A.; Cui, J.; Myshakin, E. M.; Duncan, M. A.; Johnson, M. A.; Jordan, K. D. Science 2005, 308, 1765.
44. Botti, A.; Bruni, F.; Imberti, S.; Ricci, M. A.; Soper, A. K. J Mol Liq 2005, 117, 77.
45. Vuilleumeir, R.; Borgis, D. Isr J Chem 1999, 39, 457.
46. Kornyshev, A. A.; Kuznetzov, A. M.; Spohr, E.; Ulstrup, J. J Phys Chem B 2003, 107, 3351.
47. Kerdcharoen, T.; Liedl, K. R.; Rode, B. M. Chem Phys 1996, 211, 313.
48. Tongraar, A.; Liedl, K. R.; Rode, B. M. J Phys Chem A 1997, 101, 6299.
49. Tongraar, A.; Liedl, K. R.; Rode, B. M. J Phys Chem A 1998, 102, 10340.
50. Tongraar, A.; Sagarik, K.; Rode, B. M. J Phys Chem B 2001, 105, 10559.
51. Schwenk, C. F.; Loeffler, H. H.; Rode, B. M. J Chem Phys 2001, 115, 10808.
52. Tongraar, A.; Sagarik, K.; Rode, B. M. Phys Chem Chem Phys 2002, 4, 628.
53. Tongraar, A.; Rode, B. M. Chem Phys Lett 2004, 385, 378.
54. Rode, B. M.; Schwenk, C. F.; Tongraar, A. J Mol Liq 2004, 110, 105.
55. Tongraar, A.; Rode, B. M. Chem Phys Lett 2005, 403, 314.
56. Intharathep, P.; Tongraar, A.; Sagarik, K. J Comput Chem 2005, 26, 1329.
57. Xenides, D.; Randolf, B. R.; Rode, B. M. J Chem Phys 2005, 122, 174506.
58. Brooks, B. R.; Bruccoleri, R. E.; Olafson, B. D.; States, D. J.; Swaminathan, S.; Karplus, M. J Comput Chem 1983, 4, 187.
59. Dunning, T. H., Jr.; Hay, P. J. In Modern Theoretical Chemistry, Vol. 3; Schaefer, H. F., Ed.; Plenum: New York, 1976.
60. Hay, P. J.; Wadt, W. R. J Chem Phys 1985, 82, 270.
61. Boys, S. F.; Bernardi, F. Mol Phys 1970, 19, 553.
62. Bopp, P.; Jancsó, G.; Heinzinger, K. Chem Phys Lett 1983, 98, 129.
63. Stillinger, F. H.; Rahman, A. J Chem Phys 1978, 68, 666.
64. Frisch, M. J.; Trucks, G. W.; Schlegel, H. B.; Scuseria, G. E.; Robb, M. A.; Cheeseman, J. R.; Zakrewski, V. G.; Montgomery, J. A.; Stratmann, R. E.; Burant, J. C.; Dapprich, S.; Millam, J. M.; Daniels, A. D.; Kudin, K. N.; Strain, M. C.; Farkas, O.; Tomasi, J.; Barone, V.; Cossi, M.; Cammi, R.; Mennucci, B.; Pomelli, C.; Adamo, C.;

Clifford, S.; Ochterski, J.; Peterson, G. A.; Ayala, P. Y.; Cui, Q.; Morokuma, K.; Malick, D. K.; Rabuck, A. D.; Raghavachari, K.; Foresman, J. B.; Cioslowski, J.; Ortiz, J. V.; Stefanov, B. B.; Liu, G.; Liashenko, A.; Piskorz, P.; Komaromi, I.; Gomperts, R.; Martin, R. L.; Fox, D. J.; Keith, T.; Al-Laham, M. A.; Peng, C. Y.; Nanayakkara, A.; Gonzalez, C.; Challacombe, M.; Gill, P. M. W.; Johnson, B. G.; Chen, W.; Wong, M. W.; Andres, J. L.; Head-Gordon, M.; Replogle, E. S.; Pople, J. A. Gaussian 98; Gaussian: Pittsburgh, PA, 1998.

65. Dunning, T. H., Jr. J Chem Phys 1989, 90, 1007.
66. Kendall, R. A.; Dunning, T. H., Jr.; Harrison, R. J. J Chem Phys 1992, 96, 6769.
67. Woon, D. E.; Dunning, T. H., Jr. J Chem Phys 1993, 98, 1358.
68. Adams, D. J.; Adams, E. H.; Hills, G. J Mol Phys 1979, 38, 387.
69. Triolo, R.; Narten, A. H. J Chem Phys 1975, 63, 3624.
70. Almlof, J. Chem Scr 1973, 3, 73.
71. McQuarrie, D. A. Statistical Mechanics; Harper and Row: New York, 1976.
72. Kreuer, K. D.; Rabenau, A.; Weppner, W. Angew Chem Int Ed Engl 1982, 21, 208.
73. Kreuer, K.; Paddison, S. J.; Spohr, E.; Schuster, M. Chem Rev 2004, 104, 4637.
74. Hofer, T. S.; Tran, H. T.; Schwenk, C. F.; Rode, B. M. J Comput Chem 2004, 25, 211.